Nonlinear Longitudinal Combustion Instability: Influence of Propellant Composition

A. K. ROBERTS* AND W. G. BROWNLEE†
Defence Research Establishment Valcartier, Valcartier, Quebec, Canada

Current stability criteria for longitudinal combustion instability were tested for generality using data from 54 different propellants. These included formulations containing polyurethane and carboxyl-terminated polybutadiene binders, ammonium perchlorate, aluminum, and rate modifiers. The propellants were tested at 70°F in 4- and 8-in. diam, tubularly-perforated motors which were pulsed to initiate the instability. It was found that for a particular propellant system, well-defined behavioral trends could be established as the formulation was varied. A considerable variability in such trends was observed, however, for grossly different propellant systems. Consequently, a generalized correlation of motor behavior with the details of propellant formulation was not achieved. Similarly, the stability criterion proposed by Capener, Dickinson, and Kier, which features a power law relation between a "threshold" burning rate and the corresponding chamber pressure, was found to be invalid in the general case.

Nomenclature

08080	= nominal 8-in. diam × 80-in. long motor
04034	= nominal 4-in. diam × 34-in. long motor
05008	= nominal 5-in. diam × 8-in. long motor
AP	= ammonium perchlorate
CTPB	= carboxyl-terminated polybutadiene
PU	= polyurethane
d_t	= diameter of nozzle throat
f	= frequency
f_w	= fraction of web thickness consumed
H	= ratio of port area to nozzle throat area ($= 1/J$)
K_n	= ratio of burning surface area to nozzle throat area
n	= ballistic parameter in burning rate law $r = \alpha P_s^n$
P_c	= chamber pressure
P_{ac}	= peak-to-peak wave pressure during head-end reflection
P_s	= stable chamber pressure
$\bar{P}_{us}$	= time-averaged pressure during unstable operation
$(P_{ac} + \bar{P}_{us})/\bar{P}_{us}$	= wave strength at head-end reflection
P_{cr}	= critical pressure
P_{tr}	= transition pressure
r	= linear burning rate of propellant during stable nonerosive operation
r_{1000}	= stable burning rate (nonerosive) at 1000 psia
r_{cr}	= stable burning rate (nonerosive) at the critical pressure
r_{tr}	= stable burning rate (nonerosive) at the transition pressure
ΔP	= jump in time-averaged pressure when transition occurs from stable to unstable operation
$\Delta P/1200$	= severity of instability when transition to unstable operation occurs at 1200 psia
$\Delta P/1400$	= severity of instability when transition to unstable operation occurs at 1400 psia

Received June 9, 1969; presented as Paper 69-480 at the AIAA 5th Propulsion Joint Specialist Conference, U.S. Air Force Academy, Colorado, June 9–13, 1969; revision received June 19, 1970.

* Leader, Ballistics Group, Propulsion Division.
† Director, Propulsion Division. Member AIAA.

Introduction

NONLINEAR longitudinal combustion instability in solid-propellant rocket motors has proved to be a rather more intractable problem than instabilities associated with the transverse modes of oscillation. In the latter case the addition of powdered aluminum to propellant formulations generally provides a solution, whereas in the former a remedy of comparable simplicity has not been forthcoming. Moreover, despite extensive efforts on the part of many investigators, a satisfactory fundamental description of longitudinal instability is not yet at hand.

Typical experimental studies oriented towards a basic understanding have been reviewed by Price[1,2] and theoretical approaches by Hart and McClure.[3] Unlike such studies, which generally attempt to elucidate a particular feature such as the response of the combustion zone to pressure fluctuations, the investigations reported here are concerned with the unstable operation of complete motor systems in typical end-vented configurations. As such, they are much less amenable to analysis aimed at basic insights but might be expected to offer useful guidelines to the motor designer. It will be shown, however, that the predominant influence of propellant composition precludes the generalization of behavioral trends observed with any particular propellant system.

That reproducible and well-defined phenomenological trends can be obtained for a particular propellant system was first demonstrated by Brownlee.[4] In these studies a very limited variety of ammonium perchlorate-polyurethane formulations were investigated. Emphasis was placed on delineating characteristic features of the instability and on determining the influence of motor geometry. It was shown that the instability is dependent on the cyclical propagation of a strong gaseous compression wave along the internal cavity of the motor. That this wave can exist at shock strength was subsequently demonstrated by Brownlee and Kimbell using a windowed rocket motor to which schlieren techniques were applied.[5] During unstable operation the interaction of the wave with the combustion processes caused the time-averaged burning rate, chamber pressure and thrust to be greater than their corresponding quasi-steady values.

It was also shown that the instability is nonlinear with respect to initiation; consequently a finite flow disturbance is ordinarily required to cause transition to the unstable mode

of operation. Because of this nonlinearity, motors capable of the most catastrophic behavior were observed to operate stably unless triggered by a naturally occurring event.[4,6–9] To overcome the experimental difficulties associated with random natural initiation and to provide a means of testing development motors, a multiple-pulse technique which employs small gun powder charges was developed.[4,6,7] It was observed that naturally and artificially triggered motors behaved identically shortly after the initiation transient.

A further result indicated the possibility of establishing stability criteria. It was found that for a given propellant formulation and grain geometry the instability could be triggered only when the chamber pressure exceeded a particular level. This and related observations led to prediction methods which will be compared with our present techniques in a later section.

The variations in polyurethane propellant formulations first studied[4] were later systematically augmented by the authors.[8] More recently, further data have been accumulated on the behavior of both polyurethane and carboxyl-terminated polybutadiene propellants. Although not systematically related in every instance, over 50 formulations have been investigated in all, each containing ammonium perchlorate as the oxidizer. These included eight binder levels from 16 to 30% by weight, 12 aluminum levels from 0 to 22% by weight, various oxidizer particle size distributions, and in some instances the rate modifiers copper chromite, ferric oxide, silica, and lithium fluoride.

Aside from the investigations just discussed, the only comparable study was carried out by Capener, Dickinson, and Kier.[10,11] Using the techniques described in Ref. 4, they obtained a surprisingly simple relationship between a so-called threshold burning rate and a threshold pressure for diverse propellant formulations. As will be seen, this simple stability criterion is not confirmed by our results.

Experimental Technique

The experimental arrangement for motor firings was identical to that described in Ref. 4 with the exception that the high-frequency response pressure gages mounted in the head plate of each motor were the improved Kistler 701A model. All motors were fired at a nominal grain temperature of 70°F. Two sizes of radial burning motors were used; motor nomenclature, perforation (port) diameters and grain lengths are given in Table 1. The grains were case-bonded and their planar ends inhibited against burning. Most 08080 motors were fired using a rupture diaphragm adaptor between the casing and the nozzle. This introduced a 5-in. diam, × 6-in. long inert channel between the grain port and the nozzle entrance. As noted in Ref. 4, no change in 08080 motor behavior was observed for motors fired without this device; all 04034 motors were fired without a safety adaptor. For both types of motors the de Laval nozzle had very short entrance sections consisting of a radiused surface which blended smoothly into a short (<0.5 in.) parallel throat section; expansion cones were conical.

Nonerosive burning rate data for stable operation at 70°F were obtained from firings of 5-in. diam × 8-in. long radial burning motors (05008). With few exceptions these motors were either cast from the same propellant mix as the larger motors or from mixes containing the same lots of raw ingredients.

Table 1 Tubular grain dimensions[a]

Motor size	D_{pi}, in.	D_{pf}, in.	L_p, in.	L_p/D_{pi}
08080	4.04	7.65	78.8	19.5
04034	1.70	3.68	33.8	19.9

[a] D_p = perforation diameter (initial and final). L_p = grain length.

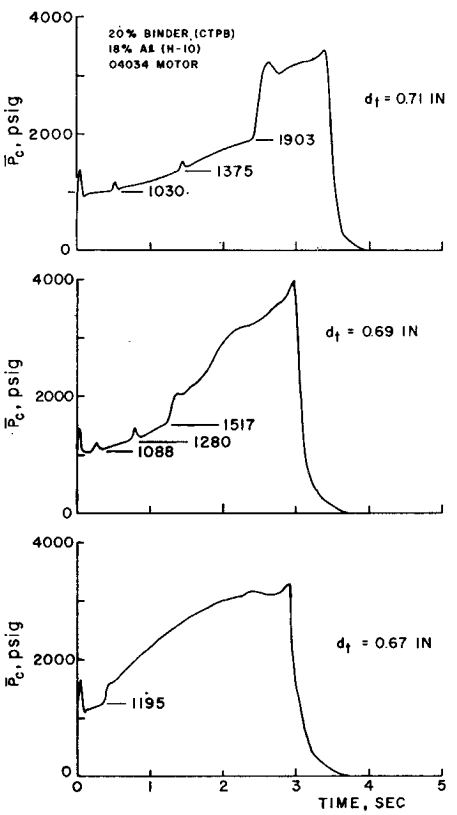

Fig. 1 Effect of reducing the throat diameter upon the onset of instability (Propellant 54 of Table 3).

In order to establish the unstable behavior of each propellant formulation under given test conditions, at least three or four motors of one type, all pulsed, were required. Two distinct classes of experimental data are obtained from such tests. In the first instance it is known that once operating unstably, the behavior of a particular motor does not depend on the detailed nature of the initiation process.[4,8] Consequently, correlations of subsequent motor behavior with variations in geometry, propellant formulation, etc., can be carried out with confidence. On the other hand, because of the nonlinear initiation mechanism noted earlier and described in detail in Ref. 4, the initiation of the instability depends crucially on the technique used to produce flow disturbances within the motor.

The technique used here and by Capener et al.,[10,11] leads to the explosive injection of high-pressure gases and burning gun powder particles through a small hole in the head plate of the motor. This is unlikely to be comparable in effect to, say, the passage of solid material down the conduit and through the nozzle, as might occur naturally. Consequently, failure to initiate instability by means of the pulse technique does not entirely guarantee that naturally initiated instability cannot occur. Nevertheless, pulse charge sizes can be optimized in the light of previous experiments and experience so as to ensure that initiation will occur, if it is possible to achieve at all using the pulse technique. In the present experiments care was taken to optimize both the charge sizes and the timing of the pulses, the former ranging from 0.3 to 1.0 g for the 04034 motors and from 1.0 to 12 g for the 08080 motors. Both the timing of the pulses and their sizes were adjusted from firing to firing so as to determine the lowest operating pressure at which initiation of the instability could be achieved.

Experimental Results

Pressure-time traces from a series of unstable firings of the 04034 motor are shown in Fig. 1. The pressure recording

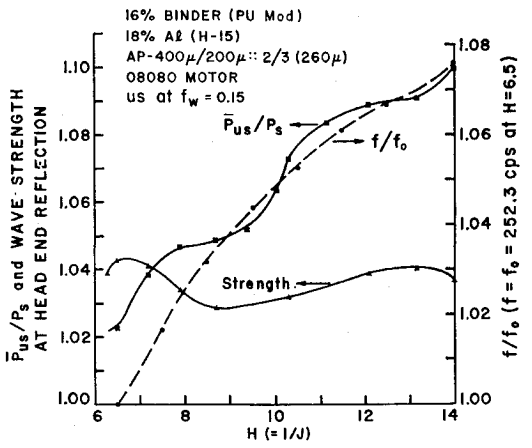

Fig. 2 Typical unstable operation of a 08080 motor (Propellant 34 of Table 3).

system was electromechanically damped so that the time-averaged pressure was displayed during periods of instability. The small disturbances on the upper traces resulted from the damped oscillations induced by pulsing.

As the nozzle throat diameter d_t was reduced from firing to firing, the motor became unstable earlier in the firing and at lower operating pressures. If d_t had been further reduced the motor would typically have become unstable on ignition. This general trend was observed for all formulations tested, no "stable" propellants being found.

Further details of unstable (US) operation are given in Fig. 2 where a number of variables for a particular 08080 firing are plotted against the ratio of port area to throat area, $H(= 1/J)$. The ratio of the time-averaged pressure during unstable operation to its equivalent value obtained from a stable firing $\bar{P}_{us}/P_s$ increased monotonically with H; that the percentage jump in pressure at transition increases with operating pressure level is also readily seen in Fig. 1. The frequency of oscillation increased slightly during this firing and all others. It can be shown that the through-flow velocity gradient acts to lower the frequency below its zero-flow value. Since the gradient becomes less severe with increasing H, the frequency would be expected to increase provided that the wave strength does not diminish appreciably.

Because heat transfer to the Kistler gages caused shifting of their base lines, the wave strength was defined as $(P_{ac} + \bar{P}_{us})/\bar{P}_{us}$ where P_{ac} is the peak-to-peak wave pressure during head-end reflection and the time-averaged pressure $\bar{P}_{us}$ has been substituted for the true minimum pressure with little

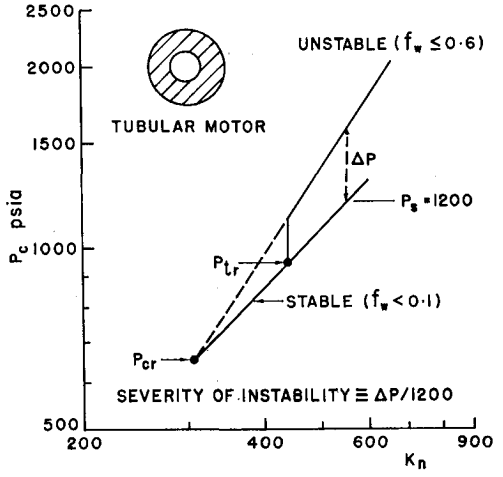

Fig. 3 Correlation of stable and unstable pressures.

Table 2 Influence of scaling on wave strength and frequency

Motor	Wave strength (18% Al) 16% Binder	Wave strength (18% Al) 17% Binder	Frequency (H = 8), cps
08080	1.02–1.04	1.03–1.05	257
04034	1.06–1.09	1.06–1.08	627

error. It is seen in Fig. 2 that the variations in the wave strength were small but were directly related to changes in the ratio $\bar{P}_{us}/P_s$. As noted in greater detail in Ref. 4, the wave strength is little influenced by changes in the throat or port diameters during a firing, or from firing to firing when a much greater range of H can be explored by choice of d_t.

The variations in wave strength seen in Fig. 2 are probably associated with the so-called humping effect.[4] This name was derived from the humped pressure-time curves which seem to be generally associated with composite propellants and of which an example may be seen in the stable portion of the upper trace of Fig. 1. Detailed analysis shows that at constant pressure the burning rate is a function of the radial web position and is generally highest at the mid-point. Consequently the coefficient α and the exponent n in the rate law

$$r = \alpha P_s^n \qquad (1)$$

are weak functions of the fraction of web burnt f_w and vary continuously. Because of the related physical variations in the propellant, it is expected that the interaction of the pressure wave with the combustion zone and any related effects should depend on f_w. This factor will be accounted for in subsequent use of such data.

Stability Criteria

It is clear that the transition to unstable operation is governed in some way by the motor geometry and/or the operating pressure. In Ref. 4 it was shown that the chamber pressure during both stable and unstable operation could be correlated with the ratio of the burning surface area to the throat area K_n. No other dependence was found, as was confirmed by Capener et al.[11] This correlation is shown diagrammatically in Fig. 3 where the coordinates are $\log P_c$ vs $\log K_n$.

In this type of plot the straight lines which correspond to stable and unstable operation are obtained from a series of three or four firings. Because of the humping effect, data for stable operation are taken at $f_w \leq 0.1$. It was found that data for unstable operation plotted essentially linearly if restricted to $f_w \leq 0.6$. In general, the slope of the upper line exceeds that of the lower so that the lines intersect at some value of P_c and of K_n. In earlier work[4,8] these values were defined as "critical" and were used as stability criteria as well as for comparing propellants. The "threshold pressure" used by Capener et al.[10,11] was obtained in this manner. More recently we have found that for many formulations the slopes differ so little that the intersection occurs at unrealistically low pressures. Moreover, in several instances instability could be induced only at pressures much exceeding the so-called critical or threshold pressure. In the present paper, therefore, we define a particular transition pressure, P_{tr}, for $f_w \simeq 0$. This pressure is determined independently of the type of plot shown in Fig. 3 by plotting the pressure at which pulsing occurred against f_w. When this is done for several motors, a line of demarcation can readily be drawn between points corresponding to the stable and unstable pulses. This line, when extrapolated to $f_w = 0$, yields P_{tr}. Evidently P_{tr} approximates the minimum operating pressure at which a particular motor can be driven unstable at ignition.

The $\log P_c$ vs $\log K_n$ plot remains useful, nevertheless, when comparing propellants since the percentage increase in

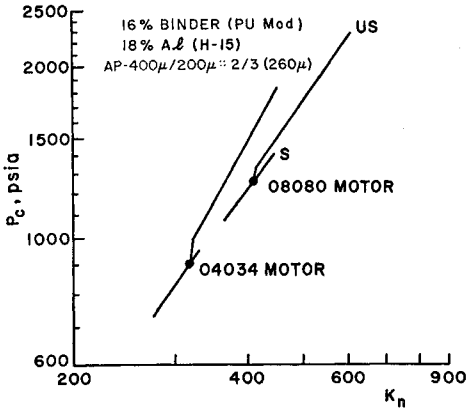

Fig. 4 Influence of motor size on transition pressure.

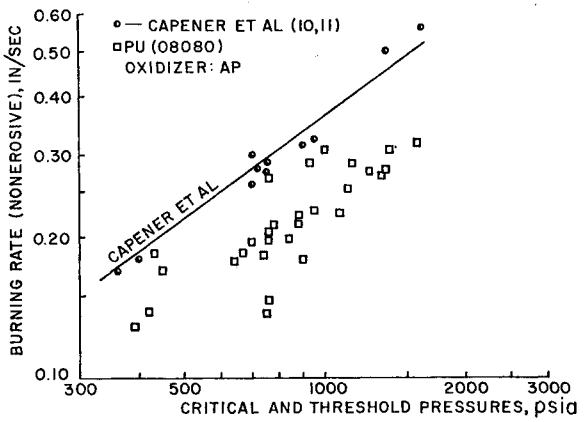

Fig. 5 Comparison of 08080 motor critical data and 05040 motor threshold data (see Table 3).

pressure as a result of transition is of considerable interest to the designer. In particular, a comparison at constant transition pressure is pertinent if stability considerations govern the selection of a propellant from otherwise suitable candidates. We therefore define the severity of instability as the ratio of the jump in pressure at transition ΔP to the pressure from which transition occurred and choose the latter at a convenient value, usually 1200 psia, as shown in Fig. 3.

Scaling Effects

Both the transition pressure P_{tr} and $\Delta P/1200$ depend on motor size as is shown in Fig. 4, where data from 04034 and 08080 motors are compared. Typically the smaller of the two motors transitioned at a lower pressure than the larger and was much more severely unstable at given pressure, in agreement with Ref. 4. A second propellant, identical to the first except for binder content, behaved similarly. In both instances the wave strength was appreciably greater in the smaller motor as shown in Table 2. In view of these substantial changes in behavior it follows that quantitative comparisons between propellants must be confined to data obtained from a particular motor configuration.

Comparison of Stability Data: Critical Pressures and Burning Rates

In the work of Capener et al.,[10,11] 25 formulations were tested of which 15 were composite propellants (14 PBAN, 1 PU) containing only ammonium perchlorate as oxidizer. The PBAN propellants can be classified into two groups, one with 16.8% of binder and 15% of aluminum (8 formulations) and the other with 20% of binder and no aluminum (6 formulations). Variations were obtained by changing the particle size distribution of the oxidizer and the aluminum type and by the addition of burning rate modifiers. These formulations were tested in a 5 in. × 40 in. (05040) radial-burning motor.[10] Critical or threshold pressure data were obtained by the intersection method described earlier. The corresponding threshold burning rate was obtained from strand burner results.[10] Two formulations were listed as being stable in the pressure range 400 to 2500 psia. Data for 11 of the remaining 13 were plotted logarithmically as shown in Fig. 5 and taken to define a linear stability boundary. Capener et al. concluded that "this bound is uniquely determined by the relationship between the pressure at which a given propellant can be driven unstable and the associated propellant linear burning rate."[11]

Also shown in Fig. 5 are 08080 data for 29 of the 54 propellants tested in the present program. In particular, these 29 propellants, all polyurethane, are those for which it was possible to obtain well-defined values of the critical (threshold) pressure by the intersection method. Table 3 gives the formulation, burning rate, $\Delta P/1200$, transition pressure, and the transition burning rate as determined from 05008 motor firings, for each of the 54 propellants, and the corresponding values of the critical pressure and the critical burning rate as plotted in Fig. 5.

In comparing the sets of data in Fig. 5 it should be noted that two different motor geometries, 05040 and 08080, were used by the investigators. No particular importance should therefore be attached to the relative shift between our data and that of Capener et al. A striking and relevant difference, however, is that our data fail to correlate linearly. At given pressure a broad range of "critical" burning rates exist. This result cannot be ascribed to uncertainties in the critical pressure values since these are known with an accuracy of at least ±5%. Moreover, the burning rates were only weakly dependent on their corresponding pressures because the rate exponent n was <0.5 in every instance.

In view of the foregoing, it seems evident that the conclusion reached by Capener et al. was based on insufficient experimental data and is, in the general case, invalid. It seems possible that their correlation was arrived at fortuitously as a result of the particular formulations studied. Alternatively, it may be that PBAN and PU propellants behave quite differently, although if this argument is used it is necessary to disregard Capener's second lowest data point which is for a PU propellant, and to restrict the generality of their conclusion.

Finally, it is worth noting that in the broadest sense, faster burning propellants tend to have higher critical pressures as was pointed out in Refs. 4 and 8.

Transition Pressures and Burning Rates

Transition data for the 54 formulations listed in Table 3 are plotted in Fig. 6. The data of Capener et al. are plotted

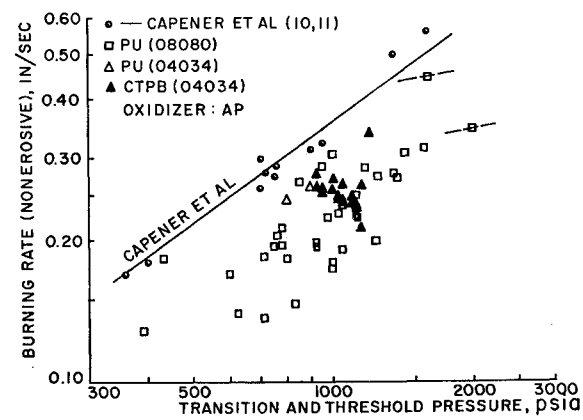

Fig. 6 08080 and 04034 motor transition data (see Table 3).

Table 3 Propellant formulations and unstable ballistic parameters, T_p = 70°F

Propellant	Motor size	Binder Type	Binder % Wt	Aluminum Type[c]	Aluminum % Wt	Oxidizer, AP Distribution	Oxidizer, AP Size, μ[d]	Oxidizer, AP % Wt	Rate modifier Type	Rate modifier % Wt	r_{1000}, in./sec	P_{tr}, psia	r_{tr}, in./sec	P_{cr}, psia	r_{cr}, in./sec	$\Delta P/1200$
01	08080	PU	25	...	...	Bimodal	150	75	...	...	0.190	430	0.185	430	0.185	0.77
02	08080	PU	25	SAX-3	5	Bimodal	150	70	...	...	0.202	775	0.197	760	0.197	0.79
03	08080	PU	25	SAX-3	5	Bimodal	150	70	LiF	1.8(added)	0.150	390	0.129	390	0.129	2.57
04	08080	PU	22	SAX-9	19	Bimodal	150	59	...	...	0.195	750	0.195	700	0.195	0.31
05	08080	PU	25	SAX-9	19	Bimodal	150	56	...	...	0.141	625	0.140	420	0.138	0.43
06	08080	PU	25	SAX-9	18	Bimodal	150	56.5	CuC	0.5	0.198	925	0.195	740	0.183	0.24
07	08080	PU	25	SAX-9	18	Bimodal	150	56	CuC	1.0	0.221	1125	0.227	880	0.212	0.07
08	08080	PU	25	SA-24	5	Bimodal	150	70	...	...	0.230	1025	0.230	950	0.228	0.24
09	08080	PU	20	SA-26	5	Bimodal	150	75	...	...	0.307	1000	0.307	1000	0.307	0.17
10	08080	PU	20	SA-26	10	Bimodal	150	70	...	...	0.309	1575	0.316	1575	0.316	0
11	08080	PU	20	SA-26	15	Bimodal	150	65	...	...	0.291	950	0.289	930	0.289	0.12
12	08080	PU	20	SA-26	20	Bimodal	150	60	...	...	0.272	850	0.268	760	0.268	0.10
13	08080	PU	25	SA-26	5	Bimodal	150	70	...	...	0.217	780	0.212	780	0.212	0.53
14	08080	PU	25	SA-26	10	Bimodal	150	65	...	...	0.207	760	0.204	760	0.204	0.40
15	08080	PU	25	SA-26	15	Bimodal	150	60	...	...	0.185	710	0.185	670	0.185	0.28
16	08080	PU	25	SA-26	19	Bimodal	150	56	...	...	0.172	600	0.171	450	0.170	0.23
17	08080	PU	30	SA-26	5	Bimodal	150	65	...	...	0.147	830	0.147	760	0.147	1.71
18	08080	PU	26	SA-26	17	Bimodal	150	56.5	CuC	0.5	0.192	800	0.184	640	0.177	0.21
19	08080	PU	27	SA-26	17	Bimodal	150	55	CuC	1.0	0.189	1050	0.192	...	...	0.17
20	08080	PU	22.5	SA-26	7.5	Bimodal	135[e]	70	...	...	0.237	1050	0.238	...	...	...
21	08080	PU	25	SA-26	5	Bimodal	135[e]	70	...	...	0.198	925	0.198	840	0.197	1.07
22	08080	PU	27	SA-26	17	Bimodal	135[e]	56	...	...	0.132	775	0.137	750	0.137	0.35
23	08080	PU	20	SA-26	15	Bimodal	135[e]	63	CuC	2.0	0.411	1400–1800	0.436–0.460	...	...	...
24	08080	PU	25	SA-26	5	Bimodal	135[e]	69	CuC	1.0	0.307	1800–2200	0.341–0.354	...	...	...
25	08080	PU	27	SA-26	17	Bimodal	135[e]	55.5	CuC	0.5	0.176	1000	0.176	...	...	0.13
26	08080	PU	27	SA-26	17	Bimodal	135[e]	55	CuC	1.0	0.195	1230	0.200	...	...	0
27	08080	PU	25	SA-26	5	Bimodal	135[e]	69	Fe_2O_3	1.0	0.278	1425	0.310	1375	0.307	0
28	08080	PU	25	SA-26	10	Bimodal	135[e]	64	Fe_2O_3	1.0	0.250	1375	0.273	1325	0.271	0
29	08080	PU	25	SA-26	17	Bimodal	135[e]	57	Fe_2O_3	1.0	0.220	1125	0.227	1075	0.224	0.13
30	08080	PU	27	SA-26	17	Bimodal	135[e]	55	Fe_2O_3	1.0	0.181	1000	0.181	900	0.178	0.18
31	08080	PU(Mod)[a]	17	H-15	14	Bimodal	260	69	...	...	0.270	1350	0.279	1350	0.279	0
32	08080	PU(Mod)[a]	17	H-15	18	Bimodal	260	65	...	...	0.249	1125	0.252	1125	0.252	0.08
32A	04034	PU(Mod)[a]	17	H-15	18	Bimodal	260	65	...	...	0.249	800	0.245	...	...	0.25
33	08080	PU(Mod)[a]	17	H-15	22	Bimodal	260	61	...	...	0.225	975	0.225	880	0.222	0.13
34	08080	PU(Mod)[a]	16	H-15	18	Bimodal	260	66	...	...	0.267	1250	0.276	1250	0.276	0
34A	04034	PU(Mod)[a]	16	H-15	18	Bimodal	260	66	...	...	0.267	900	0.261	...	...	0.15
35	08080	PU(Mod)[a]	17	H-15	18	Bimodal	260	64.5	Fe_2O_3	0.5	0.280	1175	0.288	1150	0.288	0.05
36	04034	CTPB	16	H-15	15	Bimodal	260	68.75	SiO_2	0.25	0.308	1200	0.340	...	...	0
37	04034	CTPB	18	H-15	17	Bimodal	370	64.5	Fe_2O_3	0.5	0.240	1050	0.245	...	...	0.25
38	04034	CTPB	16	SA-26	18	Trimodal	375	66	...	...	0.230	1125	0.237	...	...	0.23
39	04034	CTPB	16	H-10	12	Trimodal	330	72	...	...	0.268	925	0.261	...	...	0.13
40	04034	CTPB	16	H-10	15	Trimodal	330	69	...	...	0.264	950	0.258	...	...	0.13
41	04034	CTPB	16	H-10	18	Trimodal	330	66	...	...	0.247	1025	0.249	...	...	0.14
42	04034	CTPB	16	H-10	20	Trimodal	330	64	...	...	0.241	1100	0.249	...	...	0.14
43	04034	CTPB	17	H-10	12	Trimodal	330	71	...	...	0.271	1000	0.271	...	...	0.13
44	04034	CTPB	17	H-10	18	Trimodal	330	65	...	...	0.230	1150	0.240	...	...	0.23
45	04034	CTPB	18	H-10	12	Trimodal	330	70	...	...	0.259	1050	0.263	...	...	0.28
46	04034	CTPB	16	H-10	18	Bimodal	370	66	...	...	0.235	1050	0.239	...	...	0.28
47	04034	CTPB	16	H-10	18	Trimodal	360	66	...	...	0.237	1050	0.241	...	...	0.19
48	04034	CTPB	16	H-10	18	Trimodal	265	66	...	...	0.284	925	0.277	...	...	0.08
49	04034	CTPB	16	H-10	15	Bimodal	370	69	...	...	0.252	1150	0.262	...	...	0.27
50	04034	CTPB(Mod)[b]	16	H-10	18	Trimodal	330	66	...	...	0.258	950	0.254	...	...	0.15
51	04034	CTPB(Mod)[b]	18	H-10	12	Trimodal	330	70	...	...	0.258	1000	0.258	...	...	0.28
52	04034	CTPB(Mod)[b]	18	H-10	15	Trimodal	330	67	...	...	0.242	1025	0.245	...	...	0.18
53	04034	CTPB(Mod)[b]	18	H-10	18	Trimodal	330	64	...	...	0.229	1125	0.236	...	...	0.19
54	04034	CTPB(Mod)[b]	20	H-10	18	Trimodal	330	62	...	...	0.203	1150	0.215	...	...	0.22

[a] The PU binder was changed by increasing the amount of plasticizer and altering somewhat the curative ratios.
[b] A small change to the CTPB binder decreased the burning rates of propellants 50–54 (cf 41 and 50).
[c] SAX-3 (which contains 5–8% Mg), SAX-9 (which contains 12% Si), SA-24 and SA-26 are all blown grades of aluminum with average particle sizes (50% wt) of 40μ, 40μ, 7μ and 23μ, respectively. H-15 and H-10 are both spherical grades of aluminum with average particle sizes of 22μ and 15μ, respectively.
[d] Average size (50% by weight) as measured by Alpine Jet Siever.
[e] Removal of anti-caking agent and new handling procedures altered the particle size; for effect on rate compare 13 and 21.

for reference. It should be noted that both 04034 and 08080 data have been plotted; hence these data should not be directly compared because of the difference in motor geometry.

It will be recalled that the transition pressure was defined as that pressure at which a particular motor can, in fact, be driven unstable at ignition (i.e., $f_w = 0$). It is clear from Fig. 6 that the range of burning rates associated with a particular value of P_{tr} is even greater than the corresponding range for the critical pressure. Consequently, since a single-valued relationship between burning rate and pressure is not indicated, a more general approach to the problem of establishing stability criteria is required. In the present paper we report observed trends resulting from systematic formulation changes in particular propellant systems. A considerable variability in motor behavior was observed from system to system; consequently we are unable to propose an all-encompassing scheme for taking account of the influence of propellant composition.

Influence of Aluminum Content

In Fig. 7 the nonerosive burning rate for stable operation at 1000 psia, r_{1000}, the transition pressure, the wave strength and $\Delta P/1200$ are plotted as ordinate values vs the aluminum content by weight for a polyurethane propellant containing 25% of binder; these data are from 08080 motor firings. As the aluminum content was increased from 0 to 19% at the expense of oxidizer, both the wave strength and $\Delta P/1200$ decreased, the latter indicating a diminishing severity of instability at an operating pressure of 1200 psia. The transition pressure and r_{1000} reached maxima at about 5% of aluminum so that the fastest burning propellant burned stably at the highest operating pressure.

Similar data are given in Fig. 8 for a polyurethane propellant containing 17% of a modified PU binder. In comparison with that of Fig. 7, this binder contained an increased amount of plasticizer and somewhat altered curative ratios.

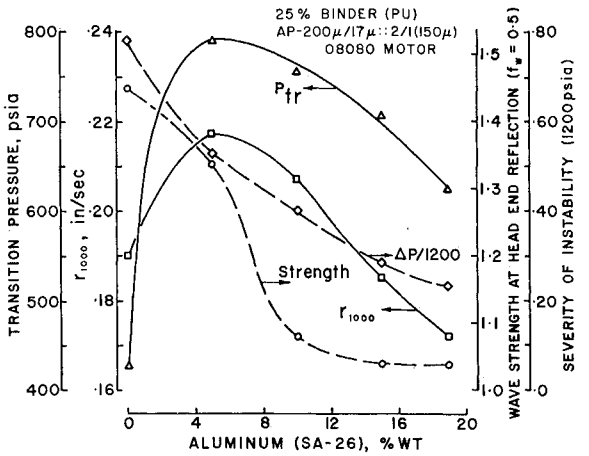

Fig. 7 Influence of aluminum content on 25% PU binder system.

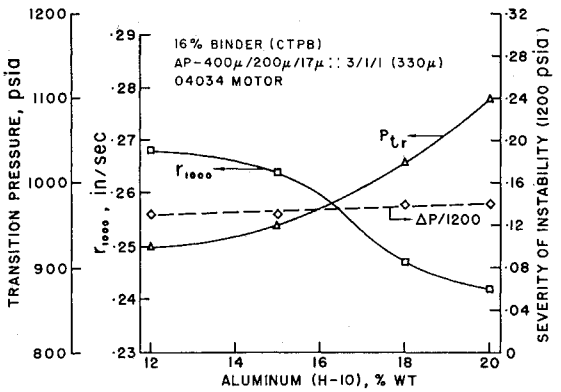

Fig. 9 Influence of aluminum content on 16% CTPB binder system.

It should also be noted that the oxidizer system was changed, the second series of formulations containing coarse AP (400 μ) and no ground (17 μ) oxidizer. The types of aluminum used were different as well, as noted in the figures.

On comparing the two series in the range 14–19% of aluminum it is seen that similar trends apply in the case of r_{1000}, P_{tr} and the wave strength, but that in the second series the severity of instability increases with aluminum content. Care must be taken when comparing the slopes of curves shown in these figures since the ordinate scales have been adjusted to better display the trends in Fig. 8.

In Fig. 9 results are shown for propellants containing 16% of a carboxyl-terminated polybutadiene binder and tested in the 04034 motor. The oxidizer was trimodal as indicated in the figure. In this series the level of aluminum content had negligible effect on the severity of instability and unlike the previous series, the transition pressure increased with aluminum level. Wave strength data are not available for the CTPB propellants.

Summarizing, the only consistent trend observed for these three propellant systems is a decrease in the stable burning rate with increasing aluminum content, hardly a novel result. It is concluded, therefore, that changes induced in the stable burning rate by formulation variations fail to provide a reliable general guide to motor behavior. This view contrasts sharply with the limited results of our earlier work where, for a particular polyurethane system, it was shown that any single formulation change which increased the burning rate also improved the stability characteristics of the propellant.[8]

Influence of Oxidizer Distribution

A series of tests was carried out in the 04034 motor with propellants containing 16% of CTPB binder, 18% of H-10 aluminum (Table 3) and various blends of oxidizer. In particular, the ratio of 400–200μ AP was held at 3:1 and the amount of 17μ AP varied. In Fig. 10 it is shown that, for this propellant system, the addition of fine perchlorate favors high burning rates and low severities of instability but also low values of the transition pressure.

In view of the diverse and conflicting trends observed when the aluminum content was varied in the three propellant systems described earlier, it would be unwise to anticipate that the trends shown in Fig. 10 have general application.

Influence of Binder Level

The influence of binder level was studied for the two greatly differing propellant systems detailed in Figs. 11 and 12. The first system was tested in the 08080 motor and contained a PU binder, 5% of SA-26 aluminum and bimodal oxidizer (150μ). The second contained a modified CTPB binder, 18% of H-10 aluminum, trimodal oxidizer (330μ) and was tested in the 04034 motor.

In both series, r_{1000} decreased with binder level while the severity of instability increased. The transition pressures, however, followed opposing trends. It is once again apparent that although a particular propellant system may exhibit well-defined behavioral trends, correlations such as have been reported here cannot be generalized to other systems. This negative result serves to emphasize the im-

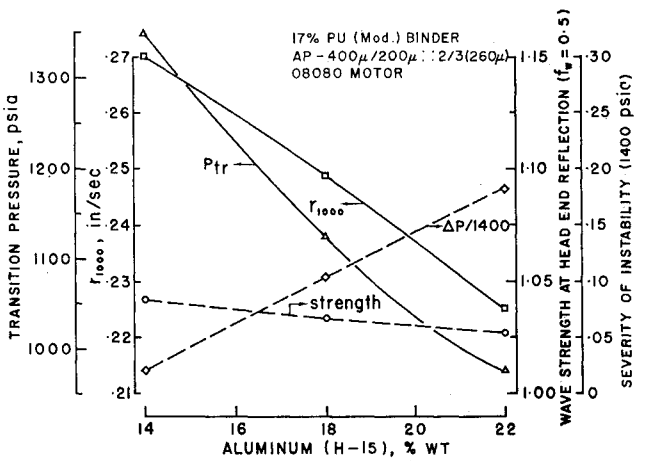

Fig. 8 Influence of aluminum content on 17% PU(Mod) binder system.

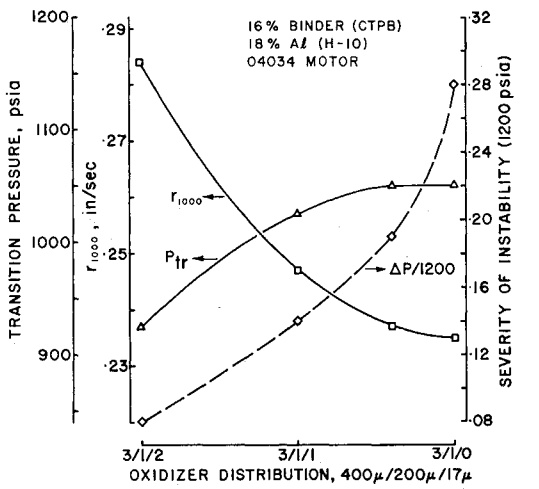

Fig. 10 Influence of oxidizer distribution.

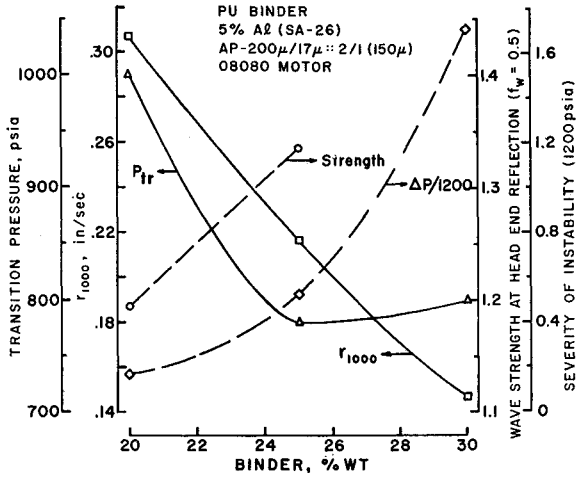

Fig. 11 Influence of PU binder level.

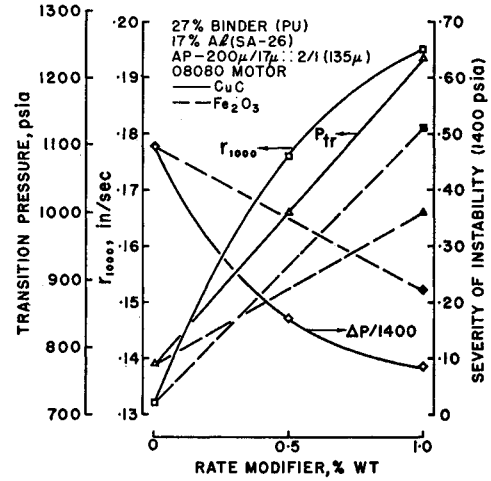

Fig. 13 Influence of rate modifiers.

portance of a detailed understanding of the fundamental processes governing the motor system.

Influence of Rate Modifiers

As a final example of the influence of formulation, Fig. 13 indicates the changes in behavior produced by incorporating rate modifiers. Two series are shown for a propellant containing 27% of a PU binder, 17% of SA-26 aluminum, bimodal oxidizer (135μ) and various amounts of ferric oxide or copper chromite. In both series the additive caused substantial rate increases, copper chromite being the more efficient of the two. Similarly, both additives caused the transition pressure to increase and $\Delta P/1400$ to decrease, very favorable trends.

Discussion

It is apparent that considerably more data are available in Table 3 than have been utilized in Figs. 7–13. Many of these data were obtained in the course of development work and are not amenable to trend analysis. A cursory examination will indicate that the severity of instability $\Delta P/1200$ cannot be uniquely related to either the stable burning rate r_{1000} or the transition burning rate r_{tr}.

The foregoing results provide little in the way of relief to the motor designer. Clearly, it is possible to investigate a particular propellant system and to establish individual trends based on selected changes to the formulation. It is also evident that such trends cannot be expected to apply to propellants containing substantially different binder or oxidizer systems.

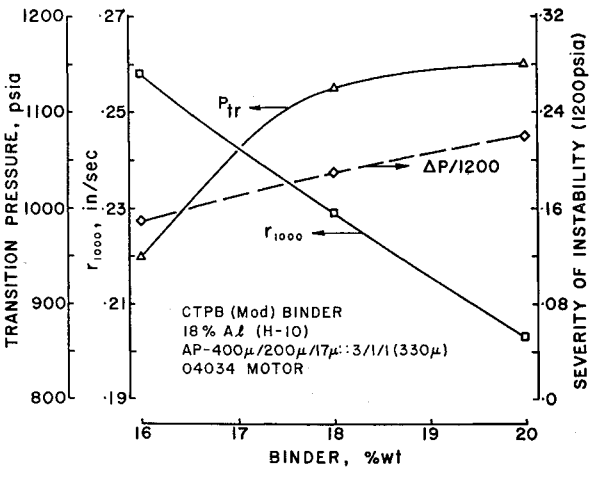

Fig. 12 Influence of CTPB(Mod) binder level.

Summary and Conclusions

The stability characteristics of 54 solid propellant formulations, which included polybutadiene and polyurethane binder systems, were evaluated in radial-burning motors. For each system studied, well-defined behavioral trends were observed when systematic variations were made in the propellant formulation. On the other hand, general trends applicable to the grossly-differing systems studied were not observed. In particular, the stable burning rate provides only a very crude indication of the relative stability of propellants.

Data from the 54 widely-differing formulations were used to test the general stability criterion proposed by Capener, Dickinson, and Kier.[11] It was concluded that their criterion is invalid in the general case.

Although only direct correlations with the details of propellant composition were attempted, the observed variability of the behavioral trends appears to preclude establishing simple guidelines for the motor designer. This result serves to underline the importance of achieving an improved understanding of the physical processes governing longitudinal combustion instability.

References

[1] Price, E. W., "Axial Mode, Intermediate Frequency Combustion Instability in Solid Propellant Rocket Motors," AIAA Paper 64–146, Palo Alto, Calif., 1964.

[2] Price, E. W., "Experimental Solid Rocket Combustion Instability," *Proceedings of the Tenth Symposium (International) on Combustion*, Univ. of Cambridge, Cambridge, England, pp. 1067–1082.

[3] Hart, R. W. and McClure, F. T., "Theory of Acoustic Instability in Solid Propellant Rocket Combustion," *Proceedings of the Tenth Symposium (International) on Combustion*, Univ. of Cambridge, Cambridge, England, pp. 1047–1065.

[4] Brownlee, W. G., "Nonlinear Axial Combustion Instability in Solid Propellant Motors," *AIAA Journal*, Vol. 2, No. 2, Feb. 1964, pp. 275–284.

[5] Brownlee, W. G. and Kimbell, G. H., "Shock Propagation in Solid-Propellant Rocket Combustors," *AIAA Journal*, Vol. 4, No. 6, June 1966, pp. 1132–1134.

[6] Dickinson, L. A., "Command Initiation of Finite Wave Axial Combustion Instability in Solid Propellant Rocket Motors," *ARS Journal*, Vol. 32, April 1962, pp. 643–644.

[7] Morris, E. P., "A Pulse Technique for the Evaluation of Combustion Instability in Solid Propellant Rocket Motors,"

Canadian Aeronautics and Space Journal, Vol. 11, No. 9, Nov. 1965, pp. 329–333.

[8] Brownlee, W. G. and Roberts, A. K., "Investigations of Nonlinear Axial Combustion Instability in Solid Propellant Rocket Motors," AIAA Paper 63-474, Cambridge, Mass., 1963.

[9] Roberts, A. K., Brownlee, W. G., and Jackson, F., "Combustion Instability and the Design of Solid Propellant Rocket Motors," *Canadian Aeronautics and Space Journal*, Vol. 16, No. 1, Jan. 1970, pp. 21–27.

[10] Dickinson, L. A., Capener, E. L., and Kier, R. J., "Propellant Deflagration Control: A Method for Suppressing Unstable Combustion," *Chemical Engineering Progress Symposium Series*, No. 61, Vol. 62, 1966, pp. 63–69.

[11] Capener, E. L., Dickinson, L. A., and Kier, R. J., "Driving Processes of Finite-Amplitude Axial Mode Instability in Solid-Propellant Rockets," *AIAA Journal*, Vol. 5, No. 5, May 1967, pp. 938–945.

JANUARY 1971 AIAA JOURNAL VOL. 9, NO. 1

A Comparison of Analysis and Experiment for Solid-Propellant Combustion Instability

M. W. Beckstead* and F. E. C. Culick†
Naval Weapons Center, China Lake, Calif.

Combustion instability data obtained with the same propellants utilizing a T-burner and an L^*-burner are presented and compared. Analyses for these burners are combined directly with results of transient analyses of the combustion. The form of the combustion analyses contains two parameters and by the proper combination of the various analyses, these two parameters can be evaluated directly in terms of the experimental variables. The results indicate the parameter values are not consistent nor necessarily realistic. It appears that the theoretical models of transient combustion result in a general, qualitative agreement with experimental data, but that extensive revisions in these models will be necessary in order to obtain quantitative agreement.

Nomenclature

a = average speed of sound
A = parameter in the response function, $A = (1 - T_i/\bar{T}_s) \times (E_s/R_0\bar{T}_s)$
A_b = admittance function defined in Eq. (16)
B = parameter in the response function, Eq. (1)
c^* = characteristic velocity, $c^* = pS_t/(\text{total mass flow})$
E_s = activation energy for surface pyrolysis
h = function defined by Eq. (14)
h_1,h_2 = functions defined by Eqs. (8e), (8f)
k = wave number, $k = (\omega - i\alpha)/a$
k_l = wave number for classical acoustic mode, $k_l = l\pi/L$
L = length of T-burner
L^* = characteristic length, $L^* = V/S_t$
m = mass flux (mass/time-area)
M_b = Mach number at the burning surface
n = index in linear burning rate law, $r \sim p^n$
n_s = index in surface pyrolysis law, $m \sim p^{n_s} \exp(E_s/R_0T_s)$
p = pressure
r = linear burning rate
R = response function, $R = R_r + iR_i$
R_0 = gas constant
$\mathcal{R}$ = universal gas constant
S_b = area of burning surface
S_c = cross-section area of T-burner
S_t = area of nozzle throat
t = time
T = temperature
T_i = initial temperature of cold propellant
T_s = surface temperature
u = speed of gas parallel to axis in T-burner
u = velocity
V = volume of L^*-burner
z = axial coordinate in T-burner
α = growth constant for acoustic waves
α_g = growth constant, Eq. (23)
α_d = decay constant, Eq. (23)
α_t = thermal diffusivity
α_1,α_2 = constants defined in Eqs. (8a), (8b)
β_1,β_2 = constants defined in Eqs. (8c), (8d)
γ = ratio of specific heats
λ = $\lambda_r + i\lambda_i$ = complex function of Ω, Eqs. (9a), (9b)
ρ = gas density
ρ_p = solid density
τ_b = characteristic time for T-burner, Eq. (30)
τ_c = characteristic time for L^*-burner, Eq. (5)
ω = angular frequency
Ω = dimensionless angular frequency, $\Omega = \alpha_t\omega/\bar{r}^2$
$(\bar{\ })$ = denotes mean value
$(')$ = denotes fluctuation

Received July 10, 1969; revision received June 11, 1970. This research is supported under NASA Work Order 6030.

* Research Chemical Engineer, Aerothermochemistry Division; now Technical Specialist, Hercules, Inc., Magna, Utah. Associate Fellow AIAA.

† Associate Professor, California Institute of Technology, Consultant to Aerothermochemistry Division. Member AIAA.

I. Introduction

In recent years combustion instability of solid propellants has been subjected to various studies, both experimental and theoretical. The experimental programs have led to the development of laboratory combustors in which unstable combustion can be studied under well controlled conditions. The most widely used and probably most versatile of these devices is the T-burner. The L^*-burner is another that has been utilized to a considerable extent recently. The research with these burners has led to experimental methods for the determination of the response of the combustion to an incident pressure perturbation. This same response is the end product of the majority of the theoretical studies. It is the purpose of the present study to compare theoretical predictions with the experimental results from a T-burner and an L^*-burner for the same propellants.

It has been shown recently[1] that virtually all of the existing linear analyses of unstable solid propellant combustion re-